

Exposure to Bleomycin, Etoposide, and Cis-Platinum Alters Rat Sperm Chromatin Integrity and Sperm Head Protein Profile 1

Authors: Maselli, Jennifer, Hales, Barbara F., Chan, Peter, and Robaire, Bernard

Source: Biology of Reproduction, 86(5)

Published By: Society for the Study of Reproduction

URL: <https://doi.org/10.1095/biolreprod.111.098616>

BioOne Complete (complete.BioOne.org) is a full-text database of 200 subscribed and open-access titles in the biological, ecological, and environmental sciences published by nonprofit societies, associations, museums, institutions, and presses.

Your use of this PDF, the BioOne Complete website, and all posted and associated content indicates your acceptance of BioOne's Terms of Use, available at www.bioone.org/terms-of-use.

Usage of BioOne Complete content is strictly limited to personal, educational, and non - commercial use. Commercial inquiries or rights and permissions requests should be directed to the individual publisher as copyright holder.

BioOne sees sustainable scholarly publishing as an inherently collaborative enterprise connecting authors, nonprofit publishers, academic institutions, research libraries, and research funders in the common goal of maximizing access to critical research.

Exposure to Bleomycin, Etoposide, and *Cis*-Platinum Alters Rat Sperm Chromatin Integrity and Sperm Head Protein Profile¹

Jennifer Maselli,³ Barbara F. Hales,³ Peter Chan,^{4,6} and Bernard Robaire^{2,3,5,6}

³Department of Pharmacology and Therapeutics, McGill University, Montréal, Québec, Canada

⁴Department of Surgery, McGill University, Montréal, Québec, Canada

⁵Department of Obstetrics and Gynecology, McGill University, Montréal, Québec, Canada

⁶McGill University Health Centre, Montréal, Québec, Canada

ABSTRACT

Testicular cancer, currently the most common cancer affecting men of reproductive age, is one of the most curable malignancies due to the progress made in the early diagnosis and effective treatment of this disease. The coadministration of bleomycin, etoposide, and *cis*-platinum (BEP) has brought the 5-yr survival rate of testis cancer patients to over 90%. However, this treatment results in reproductive chemotoxic effects. We assessed the effect of BEP treatment on sperm chromatin integrity and sperm head protein profiles of adult male Brown Norway rats following 9 wk of treatment with BEP and in animals treated for 9 wk and then subjected to a 9-wk recovery period. Both the susceptibility of DNA to denaturation and the number of strand breaks were significantly increased in mature sperm following 9 wk of treatment with BEP; proteomic analysis revealed that the expression of several proteins, including HSP90AA1 and HSP90B1, was markedly affected. Following a 9-wk recovery period, mature sperm did not show significant DNA damage, indicating that repair had potentially occurred. Interestingly, the protamination level of the sperm of these animals was significantly decreased, while histones HIST1H1D (H1.2), HIST1H4B (H4), HIST2H2AA3 (H2A1), and HIST1H2BA (H2B1A) were concomitantly up-regulated; this was not observed in the sperm immediately following 9 wk of treatment. Thus, there are persistent effects on proteins in sperm heads from the cauda epididymidis 9 wk posttreatment, in the absence of DNA strand breaks. We suggest that these effects on the sperm head proteome may contribute to long-lasting adverse effects in the progeny of BEP-exposed males.

chromatin, proteomics, spermatogenesis, testicular cancer, toxicology

INTRODUCTION

The incidence of testicular cancer, the most common cancer among young men of reproductive age, has been increasing

steadily over the past 50 yr [1, 2]. Fortunately, the mortality rate has been progressively decreasing over time as a result of early diagnosis and the advancements made in treatment protocols [1, 3]. Specifically, the coadministration of bleomycin, etoposide, and *cis*-platinum (BEP) has improved the 5-yr survival rate of testis cancer patients to over 90%, for all stages of testicular germ cell tumors [4–6]. This high cure rate, in conjunction with the young age of patients, allows many testis cancer survivors to father children after treatment. Thus, the potential negative impact of the treatment on reproductive function, fertility, and progeny outcome are of particular concern. We demonstrated previously that, in animal studies, treatment with the BEP chemotherapeutic cocktail results in decreases in reproductive organ weights, sperm count and motility, and defects in the structure of the flagella of spermatozoa [7]. Additionally, in spite of the absence of pre- or postimplantation loss, early postnatal death was significantly elevated in pups sired by BEP treated males. Drug-mediated modifications of sperm chromatin by chemotherapy may be the cause of adverse progeny outcomes.

Nuclear DNA integrity and the composition of chromatin proteins are important to normal sperm function [8]. The process of spermiogenesis, in which histones are replaced first by transition proteins and then by protamines [9], resulting in a very condensed sperm DNA structure, is absolutely critical for sperm chromatin packaging. Only a small percentage of the sperm genome remains associated with histones in mature sperm; this is approximately 15% in human spermatozoa [10] and only 1%–2% in rodent spermatozoa [11]. Recent findings have shown that the distribution of residual histones in sperm nuclei is not arbitrary but appears to be organized in a particular fashion such that their association with promoters of key gene regulators is preferentially maintained [12]. Abnormal histone retention or protamine deficiency in sperm is associated with a reduction in fertility and an increased risk of embryonic failure after fertilization [13, 14]. Besides protamines and residual histones, other sperm head proteins may be in close association with sperm chromatin and play a crucial role in normal sperm function.

We hypothesize that damage to sperm chromatin, mediated by BEP treatment, will disrupt the structure and function of sperm head proteins leading to adverse reproductive outcomes. To limit any confounding variables that may be introduced by using spermatozoa collected from human testicular cancer patients that have a diseased testis or have already undergone a cancer treatment such as orchidectomy, we used Brown Norway rats, an inbred, cancer-free animal model. To test our hypothesis we assessed the effects of BEP treatment on the sperm chromatin integrity and sperm head protein profiles of two groups of animals; the first was examined immediately following 9 wk of treatment with BEP, while the second was

¹Supported by the Canadian Institutes of Health Research (CIHR) grant (MOP-86636, to P.C.), and by the REDIH training grant from the CIHR (to J.M.)

²Correspondence: Bernard Robaire, Department of Pharmacology & Therapeutics, McGill University, 3655 Promenade Sir-William-Osler, Montréal, Québec, Canada H3G 1Y6.
E-mail: bernard.robair@mcgill.ca

Received: 20 December 2011.

First decision: 3 January 2012.

Accepted: 21 February 2012.

© 2012 by the Society for the Study of Reproduction, Inc.

This is an Open Access article, freely available through *Biology of Reproduction's* Authors' Choice option.

eISSN: 1529-7268 <http://www.biolreprod.org>

ISSN: 0006-3363

treated with BEP for 9 wk and then subjected to a 9-wk recovery period. Understanding the long-term effects of BEP exposure may have significant clinical implications for testicular cancer survivors, including the formulation of guidelines necessary to counsel survivors on the potential risk of adverse reproductive outcomes.

MATERIALS AND METHODS

Animals and Treatment

Male Brown Norway rats (4 mo of age, 12 animals per group) were purchased from Harlan (Indianapolis, IN) and housed under controlled light conditions (12L:12D) in the Animal Resources Centre of McGill University. Animals were provided with food and water ad libitum, and all experiments were conducted in accordance with the principles and procedures outlined in *A Guide to the Care and Use of Experimental Animals* prepared by the Canadian Council on Animal Care (McGill Animal Research Centre protocol 5619). Rats were treated ($n = 12$ per group) as previously described [7, 15] with a few modifications. Briefly, drug-treated animals received three cycles of 3 wk (9 wk) of the BEP regimen at a therapeutically relevant dose of 0.6 \times , with a 1 \times dose being equivalent to the human treatment regimen, as adjusted for weight and surface area. Animals were administered by gavage 1.8 mg/kg *cis*-platinum (Mayne Pharma, Montreal, QC, Canada) and 9.0 mg/kg etoposide (Novapharm, Toronto, ON, Canada) in 1 ml 0.9% saline on Days 1–5 of each week. On Day 2 of each week, rats were given an intraperitoneal injection of 0.9 mg/kg bleomycin (Bristol-Meyers, Montreal, QC, Canada) dissolved in 0.9% saline. All drugs were purchased from the Royal Victoria Hospital pharmacy (Montreal, Canada). The control animals were gavaged on Days 1–5 of each week with 1 ml of 0.9% saline. On Day 2 of each week, control rats were given 1 ml of 0.9% saline via an intraperitoneal injection.

Tissues, Chemicals, and Sperm Collection

Animals were divided into two groups such that one group ($n = 12$) of animals was euthanized by CO₂ asphyxiation and decapitation at the end of the 9-wk treatment period while the other group was euthanized 9 wk posttreatment, after the completion of one entire cycle of spermatogenesis posttreatment, during which there was no treatment. Testes, ventral prostate, and seminal vesicles were removed, weighed, and frozen in liquid nitrogen. Epididymides were removed, trimmed free of fat, weighed, and sectioned into initial segment, caput, corpus, and cauda regions. The initial segment, caput, and corpus epididymides were frozen in liquid nitrogen, while the cauda epididymides were finely minced in fresh PBS (18 mmol/L KH₂PO₄, 100 mmol/L Na₂HPO₄·7H₂O, 137 mmol/L NaCl, 27 mmol/L KCl, pH 7.4). The minced tissue was left for 5 min on ice with agitation to allow the spermatozoa to disperse and then filtered through a 70- μ m nylon strainer (BD Biosciences, Mississauga, Canada). Spermatozoa were subsequently washed three to five times with hypotonic buffer (0.45% NaCl) to lyse any contaminating cells and finally washed twice in PBS; sperm numbers were counted using a hemocytometer, aliquoted, and then frozen at –80°C until further use (see Supplemental Table S1; all supplemental data are available online at www.biolreprod.org). All chemicals were purchased from Sigma Chemical Company (St. Louis, MO), unless otherwise specified.

Comet Assay

Strand breaks in spermatozoa were evaluated using the alkaline comet assay, as previously described [16, 17] and modified by Delbès et al. [18]. Briefly, frozen sperm samples were thawed on ice and resuspended in PBS to a concentration of 1×10^5 cells/ml. Fifty microliters of the cell suspension were added to 500 μ l of molten agarose (0.5% low-melting-point grade in Mg²⁺- and Ca²⁺-free PBS, pH 7.4, at 42°C). Fifty microliters were immediately pipetted and evenly spread onto slides (Trevigen Inc., Gaithersburg, MD) in duplicate, and the gel was allowed to solidify at 4°C in the dark for 10 min. All subsequent steps were done under red light or in the dark to prevent any additional DNA damage. Slides were immersed in prechilled (4°C) lysis buffer (2.5 M NaCl, 100 mM EDTA, and 10 mM Tris-HCl; final pH 10) containing 10% dimethylsulfoxide, 1% Triton X-100, and 40 mM dithiothreitol for 1 h on ice. Following initial lysis, slides were washed in distilled water for 5 min. Proteinase K, at a concentration of 0.1 mg/ml, was added to fresh prewarmed lysis buffer, and additional lysis was done for 3 h at 37°C. Slides were washed in distilled water, placed flat at 4°C for 10 min to reset the agarose, and then immersed in freshly prepared alkaline solution (1 mM EDTA and 0.05 M NaOH, pH 12.1) for 45 min in the dark. Slides were washed twice in 1 \times Tris-

Borate-EDTA buffer (TBE, pH 7.4) for 5 min, and electrophoresis was carried out at 14 V (0.7 V/cm) for 10 min (Mini-Sub Cell GT; Bio-Rad Laboratories, Inc., Mississauga, Canada). Slides were drained and fixed in ice-cold 70% ethanol for 5 min and left to air dry prior to storage with desiccant at room temperature. DNA was stained with 50 μ l of SYBR Green solution (Trevigen) diluted 1:10 000 in Tris-EDTA buffer, pH 7.5, and analyzed using a Zeiss Axiovert 200 fully automated inverted epifluorescence microscope using a 20 \times objective. Fifty cells per slide were randomly analyzed for a total of 100 cells per animal, and images were scored for comet parameters. Tail length, percent tail DNA, and tail extent moment (tail length \times fraction of tail DNA) were measured using the KOMET 5.0 image analysis system (Kinetic Imaging Ltd., Liverpool, U.K.).

SCSA/Acridine Orange Assay

The susceptibility of sperm nuclear DNA to acid-induced denaturation was determined by the SCSA/acridine orange (AO) assay, as previously described [19]. Briefly, 200- μ l sperm samples (1×10^6 cells/ml in PBS) were thawed for 2 min at 37°C, sonicated on ice, and mixed with 400 μ l of denaturation buffer (0.08N HCl, 0.15 mol NaCl, and 0.1% Triton X-100, pH 1.4) for 30 sec at 4°C to denature uncondensed sperm DNA. After 30 sec, 1.2 ml of AO staining solution (0.126 mol Na₂HPO₄, 0.037 mol citric acid buffer, 1 mmol EDTA, 0.15 mol NaCl, pH 6.0 containing 6 μ g/ml AO) were added. Exactly 3 min after the addition of the denaturation buffer, spermatozoa were analyzed using a FACScan flow cytometer (BD Biosciences, Mississauga, Canada) fitted with an argon ion laser (488-nm line excitation). A positive control was obtained by preincubating the spermatozoa with 20 mmol H₂O₂ at room temperature for 1 h. Green fluorescence emission of AO was measured at 515–530 nm with a bandpass filter, and red fluorescence of AO was detected through a 630–650-nm long-pass filter. The raw data were processed using WinList Software (Verity Software House, Topsham, ME). The DNA fragmentation index (DFI = mean red fluorescence/total of red and green fluorescence) was analyzed according to the percentage of cells outside the main population (% DFI), and the percentage of cells with a deficiency in nuclear condensation was determined according to high-density staining (HDS), as previously described [20]. A minimum of 10 000 spermatozoa was analyzed for every sample.

Chromomycin A3 Assay

The detection of protamine deficiency in sperm chromatin was done using the flow-cytometry-based method developed by Bianchi et al. [21] and modified by Zubkova et al. [22]. Briefly, frozen sperm samples were thawed on ice, resuspended in PBS to a concentration of 1×10^5 cells/ml, and stained in chromomycin A3 (CMA3) staining solution (0.25 mg/ml in McIlvaine buffer [17 ml of 0.1 mol/L citric acid mixed with 83 ml of 0.2 mol/L Na₂HPO₄ and 10 mmol/L MgCl₂, pH 7.0]) for 20 min at 25°C in the dark. Samples were then washed twice in PBS, sonicated, and stored at 4°C in the dark until analysis. A positive control was obtained by preincubating the spermatozoa with 200 mmol dithiothreitol at 37°C for 10 min. Flow-cytometry analysis was done using a FACSAria 1 Sorter (BD Bioscience, San Jose, CA) equipped with a 407 violet solid-state laser and a 502 LP Dichroic mirror. The resulting fluorescence was detected with a 530/30 bandpass filter and quantified using BD Bioscience FACSDiva software. A minimum of 10 000 spermatozoa per sample was analyzed.

RNA Extraction and Real-Time Quantitative RT-PCR

Total RNA was extracted from testes of control and BEP-treated rats using the RNeasy Mini Plus kit with on-column DNase digestion (Qiagen, Mississauga, ON, Canada). RNA concentration was determined using the Nanodrop 2000 (Nanodrop Technologies, Wilmington, DE). Using the Roche Lightcycler (Roche Diagnostics, Laval, QC, Canada), quantitative RT-PCR was done with Quantitect One-Step SYBR Green (Qiagen) prepared according to the manufacturer's protocol, and RNA was diluted to a working concentration of 2 ng/ μ l. PCR thermal cycling parameters were 95°C for 15 min (one cycle), 94°C for 15 sec, 55°C for 30 sec, and 72°C for 30 sec (45 cycles). A standard curve for quantification was generated in each run using 0.2, 2, 10, and 20 ng/ μ l of RNA from a mixed population of spermatogenic germ cells. RT-PCR primers for *Prl1* were provided by Qiagen (SABiosciences, PP61693A), and those for *Rn18s* were designed using Primer3 software (<http://frodo.wi.mit.edu>) and provided by Alpha DNA (Montreal, QC, Canada) (forward primer 5'-CCTCCAATGGATCCTCGTTA-3'; reverse primer 5'-AAACGGCTACCACATCCAAG-3'). The expression level of the gene of interest was corrected using the endogenous control, 18S rRNA, and the relative ratio of mRNA expression per sample was determined. The results

shown are the mean of six separate rats per group with each standard and sample being analyzed in duplicate.

Immunofluorescence

To assess protamine 1 immunoreactivity, spermatozoa from the cauda epididymidis were treated as previously described [23] to remove perinuclear material. Briefly, sperm heads (1×10^6 cells/ml) were resuspended in 250 μ l of solution containing 1% SDS, 50 mM Tris-HCl, pH 7.5, 1 mM EDTA, and a protease inhibitor cocktail (Sigma, 1:100 dilution) for 10 min at room temperature and then homogenized with an ultrasonicator (Sonics & Materials Inc., Newtown, CT) for 45 sec at amplitude 15. Spermatozoa were then washed three times with 50 mM Tris-HCl, pH 7.5, and resuspended in 250 μ l of decondensation buffer (20 mM 1,4-dithiothreitol [DTT], 25 mM Tris-HCl, pH 7.5, and protease inhibitor cocktail) for 40 min at room temperature. For the immunofluorescence analysis, 50- μ l samples were placed on slides (two sample areas per slide) and left at room temperature for 20 min to allow sperm to adhere to the slides. Slides were then washed in PBS, fixed in 2% paraformaldehyde for 30 min at room temperature, and further washed in PBS, and nonspecific binding sites were blocked using PBS containing 2% normal goat serum (Vector Laboratories, Burlington, ON, Canada) and 1% BSA for 30 min at room temperature. Slides were incubated overnight at 4°C with primary antibody Hup1N monoclonal human protamine 1 (P1) antibody (kindly provided by Dr. Rodney Balhorn, Lawrence Livermore National Laboratory) diluted at 1:100 in BSA/goat serum/PBS; control sections were incubated in blocking serum alone. Slides were washed in PBS and incubated for 1.5 h in the dark at room temperature with secondary antibody solution containing Alexa Fluor 594-conjugated goat anti-mouse IgG antibody (1:200 dilution; Invitrogen) in PBS. Spermatozoa were counterstained with DAPI to stain nuclear DNA, washed, and mounted using Permafluor antifade mounting medium (Thermo Scientific, Nepean, ON, Canada). Staining was visualized on a Zeiss LSM 510 Axiovert confocal microscope using an 63/1.4 \times oil differential interface contrast objective. For quantitative analysis, at least 100 sperm per sample were analyzed using MetaMorph Imaging System software (Molecular Devices, Sunnyvale, CA).

Sperm Head Protein Extraction

Frozen sperm samples (25×10^6 cells/ml) were thawed on ice and homogenized with an ultrasonicator (Sonics & Materials Inc., Newtown, CT) for three bursts of 30 sec separated by 30-sec intervals on ice, in order to separate sperm heads from tails. Samples were then filtered twice through a 20- μ m nylon mesh and centrifuged at $13\,000 \times g$ for 10 min at 4°C to obtain a pellet that was 98% pure in sperm heads. Sperm heads were lysed, and protein was extracted, as previously described [24, 25]. Briefly, samples were incubated in a mixture containing 6 M guanidine thiocyanate (Sigma), 575 mM DTT (Invitrogen), 7 M urea (ICN Biomedicals, Aurora, OH), and 2 M thiourea (Fisher) for 15 min at room temperature. Chemicals were diluted with the addition of 165 μ l of MilliQ water followed by ultrasonication for 5 sec to lyse any remaining cells. Samples were then centrifuged at $13\,000 \times g$ for 10 min at 4°C; the supernatant was retained, and ice-cold acetone was added to each sample in a 4:1 ratio and kept at -80°C overnight to precipitate sperm head proteins and solubilize contaminants that interfere with the downstream SDS-containing applications. A final centrifugation was done at $13\,000 \times g$ for 10 min at 4°C, the supernatant was removed, and the pellet was air dried prior to being resuspended in 1 \times Laemmli buffer.

One-Dimensional Gel Electrophoresis

Sperm head protein extractions ($n = 3$ for each control and treated/group) were submitted to the McGill University and Genome Quebec Innovation Centre (Montreal, QC, Canada) to be processed for proteomic analysis. Samples (5 μ g) were resolved on a 2.4-cm one-dimensional SDS-PAGE with a 7%–15% acrylamide gradient. Proteins on the gel were stained using Coomassie Blue G. Each lane was subjected to automated band excision, to generate 15 bands per lane. The Protein Picking Workstation Pro-XCISION (Perkin Elmer, Waltham, MA) was set to excise five to seven pieces per band, depending on the width of the lane. Following transfer of the gel pieces to a 96-well tray, proteins were destained, reduced, cysteine-alkylated, and in-gel digested by automation in a MassPrep Workstation (Waters-Micromass, Milford, MA). In-gel tryptic digestion was carried out with Sequencing Grade Modified Trypsin (Promega, Madison, WI) at a final concentration of 6 ng/ μ l and allowed to incubate at 37°C for 4.5 h. Peptides were then extracted by the addition of increasing acetonitrile concentration to a final extract of 0.54% formic acid, 15.9% acetonitrile in 16 mM ammonium bicarbonate.

Liquid Chromatography/Mass Spectrometry/Mass Spectrometry Analysis

Injections of digested extracts and desalting were done using an Isocratic Agilent 1100 series Nanopump (Agilent Technologies, Mississauga, Canada). The reverse-phase peptide separation was done with a Biobasic C18 PicoFrit column (New Objective, Woburn, MA), and peptides were eluted with a gradient of formic acid and acetonitrile. The separation system was coupled to a Waters-Micromass QTOF Micro mass spectrometer set to perform tandem mass spectrometry (MS). The scan range was 350–1600 mass:charge (m/z) ratio, allowing a minimum size of 750 Da for a doubly charged peptide, approximately six amino acids in length, to an upper limit of 4800 Da for a triply charged peptide. Peptides that are too small or too hydrophilic may not be adequately retained by the column. MS/MS raw data were manipulated for the generation of peak lists, which were searched against the UniProt database using the Mascot 2.1 software. The search was limited to *Rattus norvegicus* taxonomy using carbamidomethyl cysteine as a fixed modification, methionine oxidation as a variable modification, and 0.5 Da of precursor mass and 0.5 Da of fragment mass tolerances. An additional search using X!Tandem was done on the subset database of identified proteins with additional modifications considered for D/E and c-terminal methylation, propionamide modification of C, deamidation of N/Q, and pyroglutamic acid formation of n-terminal E/Q. Using Scaffold version 3.0 (Proteome Software, Portland, OR), results were analyzed based on the spectra assigned to tryptic peptide sequences at the 95% confidence level, with a minimum of two peptides required to identify a protein and a false discovery rate lower than 0.1%. The spectral counting method was used to quantify the relative amounts of proteins among samples [26]. Data were normalized based on the unweighted spectral counts of each protein, which is the number of times a spectrum was assigned to a peptide belonging to a specific protein, and are thus expressed as quantitative values.

Western Blotting

Total protein was extracted from heads of spermatozoa obtained from the cauda epididymides of control and BEP treated rats, as described above. Protein concentrations were determined using the BioRad protein assay kit according to the manufacturer's protocol (BioRad, Mississauga, ON, Canada). Samples (20 μ g/lane) were resolved by SDS polyacrylamide (w/v) gradient (4–12%) Bis-Tris gels (Invitrogen) at 135 V for 1.5 h using MES (2-[N-morpholino] ethanesulfonic acid) SDS running buffer and then transferred onto PVDF membranes. Membranes were blocked with 5% nonfat milk in TBS containing 0.1% Tween-20. Proteins were detected using antibodies specific for H2B1A (Abcam ab1790, 1:3000), H4 (Abcam ab10158, 1:100), H1.2 (Abcam ab17677, 1:500), and H2A1 (Abcam ab13923, 1:250), all diluted in 3% nonfat milk in TBS-0.1% Tween-20 followed by HRP-linked secondary antibodies and compared with the amount of GAPDH (Abgent AP8610c, 1:100), a protein localized mainly to the principal piece of the flagellum and one of the most abundant and consistently expressed proteins across all of our samples, with a variability of less than 8% among the control and BEP-treated groups, to correct for loading (see Supplemental Figure S1, for an additional loading control).

Statistical Analyses

Statistical analyses were done using SigmaPlot 11.0 (Systat Software Inc., Chicago, IL). Results expressed as means and standard errors of the mean were analyzed using Student *t*-test.

RESULTS

BEP-Induced DNA Strand Breaks Are Decreased During a 9-Wk Recovery Period

The presence of strand breaks in BEP-treated cauda spermatozoa was evaluated using the comet assay (Fig. 1). The percentage of DNA present in the tail (Fig. 1A), the tail length (Fig. 1B), and the tail extent moment (Fig. 1C) were all significantly increased in spermatozoa of rats treated with BEP for 9 wk compared to their control counterparts. Interestingly, rats allowed a 9-wk recovery period following the 9 wk of BEP treatment showed a reversal of this effect in all three parameters compared to the control-treated animals of the same group (Fig. 1, A–C).

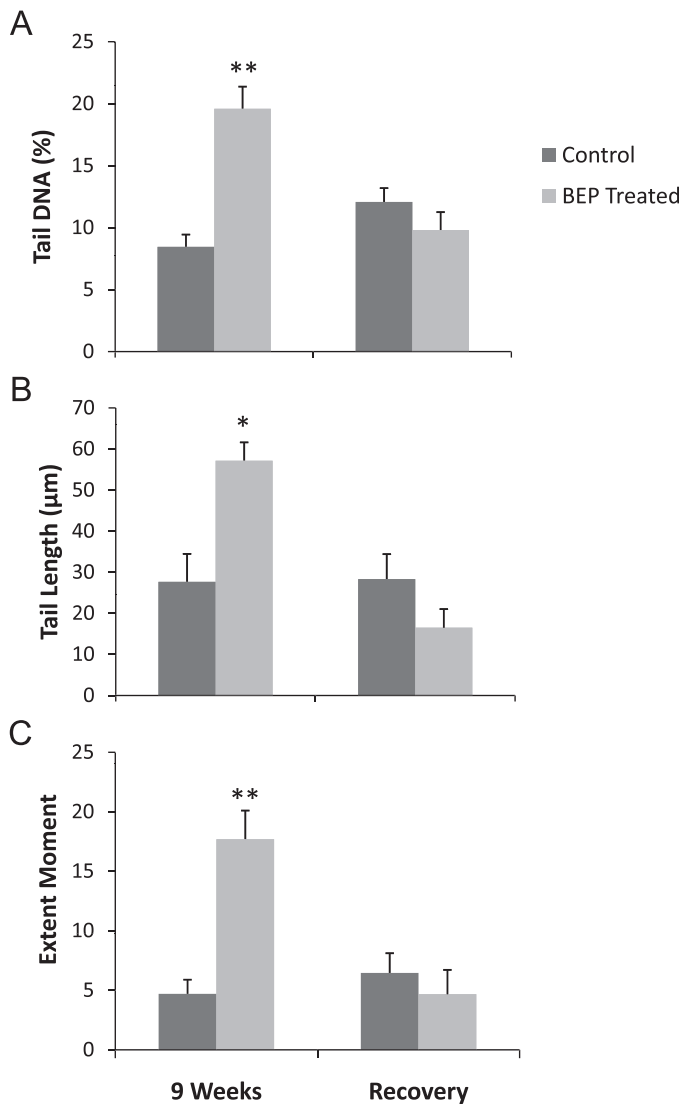


FIG. 1. Strand breaks, as evaluated by the comet assay, in cauda spermatozoa immediately following treatment with saline (control) or BEP for 9 wk or after a 9-wk recovery period. Data for % tail DNA (A), tail length (B), and tail extent moment (C) are represented as mean \pm SEM. * ($P < 0.01$) and ** ($P < 0.001$) $n = 6$.

The extent of DNA damage in spermatozoa exposed to BEP for 9 wk was further determined by assessing sperm chromatin integrity using the SCSA/AO assay (Fig. 2). The percent DNA fragmentation index (percentage of damaged cells) was significantly increased immediately after 9 wk of BEP treatment compared to that of spermatozoa following a 9-wk recovery period (Fig. 2A). High DNA stainability (HDS) was determined to understand if the damage present is a result of a poorly compacted DNA structure within spermatozoa. The percentage of cells in which AO is bound to dsDNA and fluoresces green at an intensity greater than the main population of cells is an indication of increased accessibility of the DNA structure to the dye. HDS in the spermatozoa of rats treated with BEP and allowed a 9-wk recovery period was significantly increased compared to that of spermatozoa collected from rats immediately after 9 wk of treatment (Fig. 2B). Thus, chromatin compaction/AO accessibility to DNA is dramatically affected in posttreatment spermatozoa.

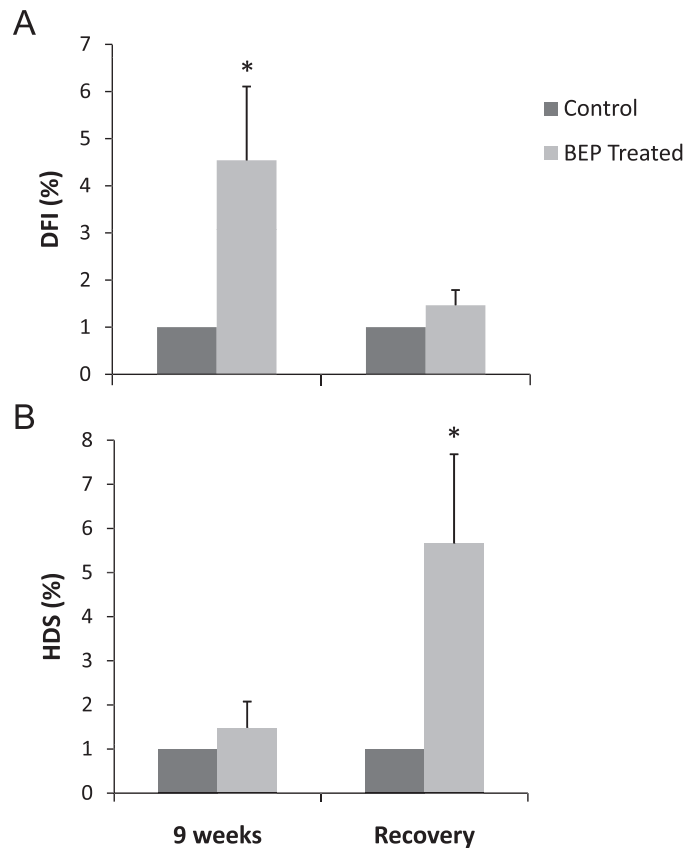


FIG. 2. Sperm chromatin structure assay (SCSA/AO assay) determined in mature cauda spermatozoa, illustrating % DNA fragmentation index (DFI) (A) and % high DNA stainability (HDS) (B), a marker of poorly condensed spermatozoa, at 9 wk and following a 9-wk recovery period in saline and BEP-treated animals. Bars represent means \pm SEM, $n = 6$. The asterisk indicates $P < 0.05$.

Effects of BEP Treatment on Sperm Chromatin Compaction as Assessed by the CMA3 Assay

The CMA3 assay indirectly determines the amount of protamine bound to the minor groove of sperm DNA. The mean CMA3 fluorescence (Fig. 3) was not altered by 9 wk of BEP treatment; however, CMA3 fluorescence was increased significantly in spermatozoa from rats treated with BEP for 9 wk followed by a 9-wk recovery period, suggesting a decrease

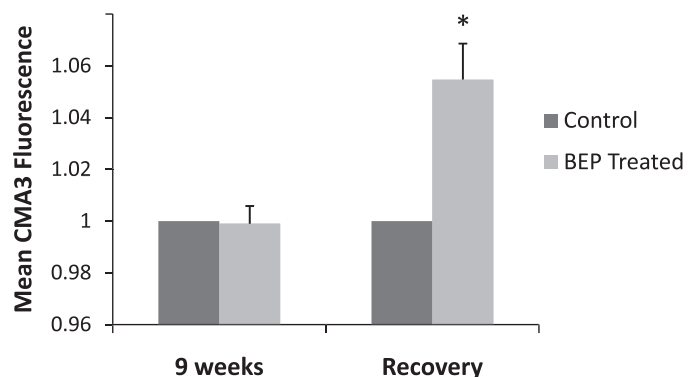


FIG. 3. Protamine content, assessed indirectly by measuring CMA3 fluorescence in spermatozoa of animals treated with saline or BEP for 9 wk versus animals subjected to a recovery period of 9 wk. Bars represent means \pm SEM, $n = 6$. The asterisk indicates $P < 0.01$.

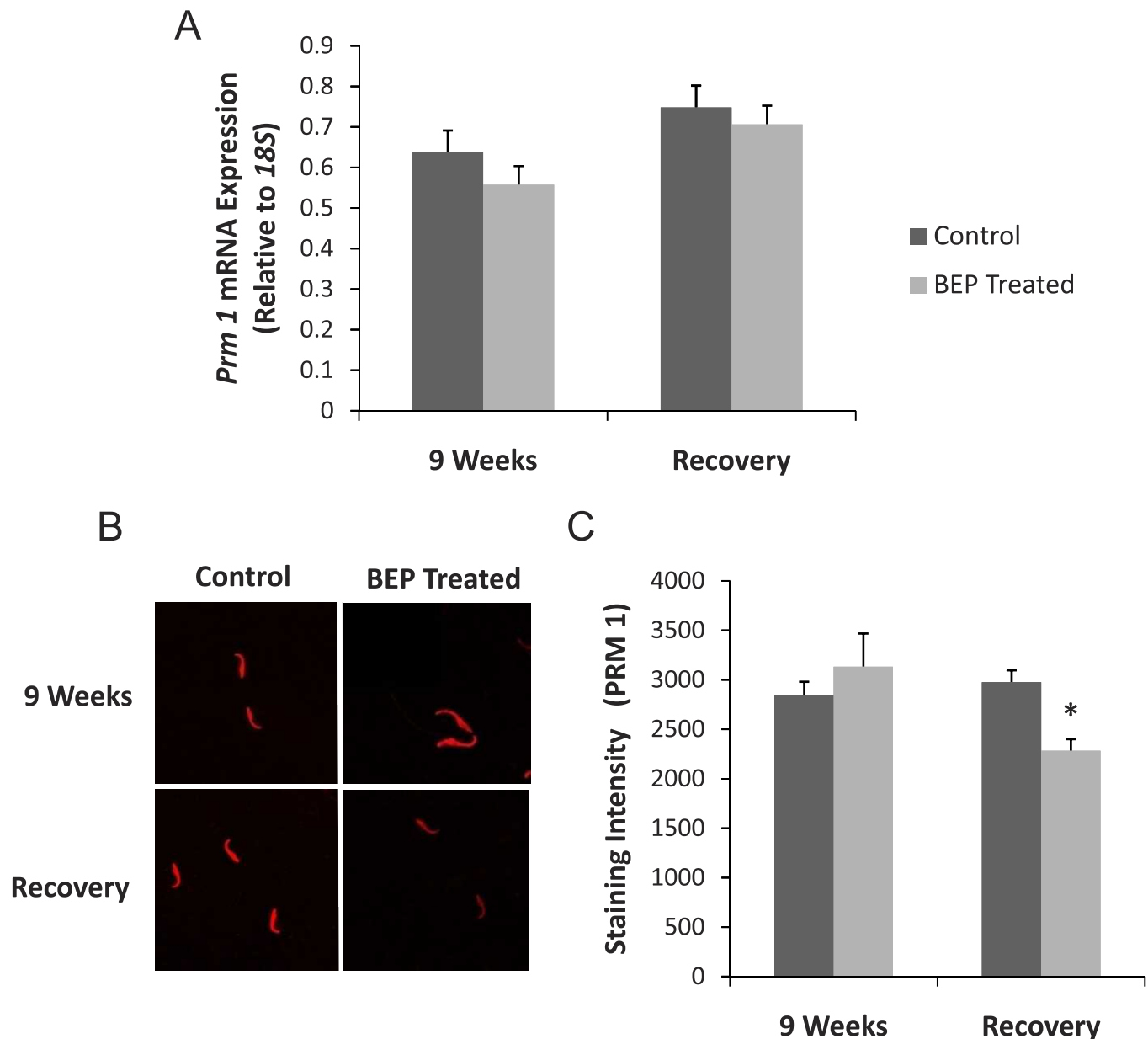


FIG. 4. Relative mRNA expression of *Prm1* (A) in testis of control and BEP-treated rats after 9 wk of treatment or following a recovery period ($n = 6$). Qualitative analysis of PRM1 (red) immunofluorescence (B) with original magnification $\times 63$. Quantitative analysis of the PRM1 staining intensity (C) in cauda spermatozoa of control and BEP-treated rats after 9 wk of treatment or following a recovery period. Bars represent means \pm SEM, $n = 4$. The asterisk indicates $P < 0.01$.

in protamine content. To further pursue the explanation for this change in CMA3 fluorescence between the two treated groups, protamine 1 (PRM1) protein expression was quantified directly (Fig. 4). *Prm1* mRNA expression levels were determined using qRT-PCR. No change in *Prm1* transcripts was detected in either the 9-wk or the recovery group following saline or BEP treatment (Fig. 4A). PRM1 immunofluorescence was found throughout the sperm nucleus in a very diffuse pattern (Fig. 4B). The spermatozoa of animals treated for 9 wk with BEP showed no apparent changes in PRM1 staining intensity, although the spermatozoa appeared somewhat elongated; this was not significant upon further analysis (Supplemental Figure S2). After a 9-wk recovery period following BEP treatment for 9 wk, spermatozoa from drug-treated animals had a statistically significant reduction in PRM1 staining intensity when compared to the control animals (Fig. 4 B and C). Thus, a

decrease in PRM1 protein expression was observed in BEP treated animals after 9 wk of recovery.

Effects of BEP Treatment and Recovery on the Proteomic Profile of Sperm Heads

A complete proteomic analysis of the rat sperm head following BEP treatment for 9 wk with and without an additional 9-wk recovery period led to the identification of 167 proteins (Supplemental Table S2). Of the proteins identified, 37 proteins were significantly changed by at least 1.5-fold in cauda epididymal sperm of animals treated with BEP for 9 wk compared to the control-treated animals of the same group (Table 1). Of these affected proteins, 27 were up-regulated, while the remaining 10 proteins were down-regulated. In cauda epididymal sperm of animals treated with BEP for 9 wk

TABLE 1. Significantly changed proteins in cauda sperm head preparations of animals treated with BEP for 9 wk.

Protein name	Protein symbol	Accession no.	9 wk		Fold change
			Control	BEP treated	
Clusterin	CLU	P05371	2.65	14.54	5.49
Heat shock protein 90, beta, member 1	HSP90B1	Q66HD0	1.00	4.18	4.18
Lipocalin 5	LCN5	P06911	1.00	3.06	3.06
Actin, beta	ACTB	P60711	1.04	3.07	2.96
Protein disulfide isomerase family A, member 3	PDIA3	P11598	1.00	2.51	2.51
Tektin 4	TEKT4	Q6AXV2	1.34	3.13	2.33
Voltage-dependent anion channel 1	VDAC1	Q9Z2L0	1.22	2.83	2.33
Lamin A	LMNA	P48679	1.00	2.05	2.05
Tektin 5	TEKT5	Q6AYH7	2.21	4.46	2.02
Heat shock protein 90, alpha (cytosolic), class A member 1	HSP90AA1	P82995	1.63	3.22	1.98
Family with sequence similarity 166, member A	FAM166A	Q4QR77	1.04	2.05	1.97
5'-Nucleotidase, cytosolic IB	NT5C1B	Q6AXN7	2.66	5.21	1.96
Diazepam binding inhibitor-like 5	DBIL5	P56702	10.38	19.83	1.91
Phosphoglycerate kinase 2	PGK2	Q5XIV1	1.22	2.30	1.89
RSB-66 protein	RSB66	Q7TSB9	2.25	4.14	1.84
Hemoglobin alpha, adult chain 2	HBA-A2	P01946	1.04	1.87	1.79
Eukaryotic translation elongation factor 1 alpha 1	EEF1A1	P62630	1.00	1.78	1.78
Fibronectin type 3 and ankyrin repeat domains 1	FANK1	Q66H07	1.93	3.42	1.77
Cytochrome c oxidase subunit IV isoform 1	COX4I1	P10888	2.85	4.97	1.74
Glutathione S-transferase omega 2	GSTO2	Q6AXV9	1.41	2.43	1.73
Peptidylprolyl isomerase A (cyclophilin A)	PP1A	P10111	1.00	1.69	1.69
Sorcin	SRI	B0BNJ1	2.85	4.65	1.63
Dihydrolipoamide S-succinyltransferase (E2 component of 2-oxo-glutarate complex)	DLST	Q01205	1.00	1.59	1.59
Keratin 8	KRT8	Q10758	1.00	1.59	1.59
Keratin 10	KRT10	Q6IFW6	1.00	1.59	1.59
Milk fat globule-EGF factor 8 protein	MFG8	P70490	1.00	1.59	1.59
Fibrous sheath CABYR binding protein	FSCB	Q4V7A4	2.75	4.28	1.56
Similar to hypothetical protein FLJ25414	RGD1359156	Q66H17	2.73	1.00	-2.73
Cytochrome c, testis	CYCT	P10715	5.51	2.37	-2.32
ATP synthase, H ⁺ transporting, mitochondrial Fo complex, subunit d	ATP5H	P31399	4.37	2.15	-2.03
Dynein, axonemal, light intermediate chain 1	DNALI1	Q4FZV3	2.43	1.27	-1.92
Serine proteinase inhibitor HongrES1	LOC299271	Q7TN19	1.84	1.00	-1.84
Histone cluster 1, H4B	HIST1H4B	P62804	16.06	8.96	-1.79
3-Hydroxyisobutyrate dehydrogenase	HIBADH	P29266	2.25	1.27	-1.78
Similar to sphingomyelin phosphodiesterase 3, neutral membrane	RGD1565316	B0BMZ4	1.78	1.00	-1.78
Cytochrome c oxidase subunit II	COX2	Q38RV9	1.77	1.00	-1.77
Dihydrolipoamide dehydrogenase	DLD	Q6P6R2	4.09	2.34	-1.75

followed by a 9-wk recovery period, the expression of 45 proteins was changed significantly by at least 1.5-fold when compared to the control animals of the same group (Table 2). Of these, 34 were up-regulated and 11 were down-regulated.

Specific Up-Regulation of Histones Following Prolonged Cessation of BEP Treatment

Interestingly, of the five histones identified in the whole sperm head proteomic analysis, histones HIST1H1D (referred to as H1.2), HIST1H2BA (referred to as H2B1A), and HIST2H2AA3 (referred to as H2A1) were found to be three of the 34 up-regulated proteins in the recovery group (Table 2). Additionally, histone HIST1H4B (referred to as H4) protein expression was found to be significantly decreased following 9wk of BEP treatment compared to the control counterparts (Table 1). Confirmation of the changes in histone protein expression was done by Western blot analysis (Fig. 5). As expected from our proteomics analysis, histones H1.2, H2B1A, and H2A1 protein levels were not significantly different from control in spermatozoa of rats treated with BEP for 9 wk; however, an up-regulation of 2.3-fold, 1.8-fold, and 2.2-fold, respectively, was observed in spermatozoa of animals treated with BEP for 9 wk followed by a 9-wk recovery period compared to the control (Fig. 5, A–C). Western blot analysis of histone H4 did not reveal the anticipated significant decrease in

protein expression following 9 wk of BEP treatment (Table 1); Figure 5D demonstrates an equivalent protein expression in both the BEP and the control-treated animals after 9 wk of treatment. However, a significant up-regulation of 2.4-fold in the BEP-treated animals following the 9-wk recovery period versus the control-treated animals of the same group was observed; this was consistent with, but more marked than, the 38% increase seen in histone H4 expression that was determined by proteomic analysis (Supplemental Table S2).

DISCUSSION

DNA damage in the form of strand breaks and increased susceptibility to acid-induced denaturation was shown in this study to be increased significantly following 9 wk of BEP treatment, indicative of the presence of extensive unrepaired damage during spermatogenesis. Previous studies, using various doses of BEP, have also demonstrated the damaging effects of a 9-wk treatment on sperm DNA integrity [18]. Despite the importance of studying the effects of drugs during treatment, it may be even more critical to assess recovery. The lack of DNA strand breaks and acid-induced denaturation in the cauda spermatozoa from animals treated with the BEP cocktail for 9 wk, followed by a 9-wk recovery period in which no treatment was administered, indicated that the subsequent generations of spermatozoa following BEP treatment may have

TABLE 2. Significantly changed proteins in cauda sperm head preparations of animals treated with BEP for 9 wk followed by a 9-wk recovery period.

Protein name	Protein symbol	Accession no.	Recovery		Fold change
			Control	BEP treated	
Heat shock protein 90, alpha (cytosolic), class A member 1	HSP90AA1	P82995	1.00	6.67	6.67
Similar to keratin complex 2, basic, gene 6a	LOC683313	Q4FZU2	1.00	2.93	2.93
Tektin 1	TEKT1	Q99JD2	1.02	2.78	2.71
Lipocalin 5	LCN5	P06911	1.02	2.73	2.67
Histone cluster 1, H1d	HIST1H1D	P15865	2.46	6.15	2.50
Calmodulin	CALM	P62161	1.02	2.55	2.49
Eukaryotic translation elongation factor 1 alpha 1	EEF1A1	P62630	1.02	2.41	2.36
Hemoglobin alpha, adult chain 2	HBA-A2	P01946	1.02	2.38	2.33
Heat shock protein 90, beta, member 1	HSP90B1	Q66HD0	1.00	2.30	2.30
Phosphoglycerate kinase 2	PGK2	Q5XIV1	1.00	2.30	2.30
Fibrous sheath CABYR binding protein	FSCB	Q4V7A4	3.10	7.08	2.28
NudC domain containing 2	NUDCD2	Q5M823	1.00	2.27	2.27
Dihydrolipoamide dehydrogenase	DLD	Q6P6R2	3.06	6.09	1.99
Actin, beta	ACTB	P60711	1.00	1.98	1.98
Solute carrier family 2 (facilitated glucose transporter), member 3	SLC2A3	Q07647	1.00	1.98	1.98
Ubiquitin c	UBC	Q63429	3.36	6.63	1.97
Keratin 1	KRT1	Q6IMF3	1.00	1.96	1.96
Sperm adhesion molecule 1 (PH-20 hyaluronidase, zona pellucida binding)	SPAM1	Q62803	2.34	4.58	1.95
Histone cluster 1, H2ba	HIST1H2BA	Q00729	14.62	28.22	1.93
Annexin A2	ANXA2	Q07936	1.02	1.96	1.91
Lamin A	LMNA	P48679	1.00	1.76	1.76
Basigin	BSG	P26453	1.00	1.74	1.74
Tektin 4	TEKT4	Q6AXV2	1.02	1.78	1.74
Tektin 2 (testicular)	TEKT2	Q6AYM2	4.17	7.12	1.71
Cytochrome c oxidase subunit, Va	COX5A	P11240	3.89	6.62	1.70
Hexokinase 1	HK1	P05708	7.95	13.30	1.67
RAB2A, member RAS oncogene family	RAB2A	P05712	1.02	1.66	1.62
Heat shock protein 4-like	HSPA4L	B4F772	1.02	1.65	1.61
NADH dehydrogenase (ubiquinone) Fe-S protein 5	NDUFS5	B5DEL8	1.04	1.67	1.60
Hemoglobin beta	HBB	P02091	4.48	7.01	1.57
Peroxisiredoxin 5	PRDX5	Q9R063	4.02	6.24	1.55
5'-Nucleotidase, cytosolic IB	NT5C1B	Q6AXN7	3.36	5.19	1.54
Histone cluster 2, H2aa3	HIST2H2AA3	P02262	11.04	17.02	1.54
Heat shock protein 2	HSPA2	P14659	8.56	12.87	1.50
Sorcin	SRI	B0BNJ1	5.45	2.21	-2.47
Adenylate kinase 2	AK2	P29410	2.11	1.01	-2.10
Glycerol-3-phosphate dehydrogenase 2, mitochondrial	GPD2	P35571	20.15	10.17	-1.98
Ubiquinol-cytochrome c reductase, Rieske iron-sulfur polypeptide 1	UQCRCF1	P20788	3.36	1.85	-1.81
Hydroxyacyl-CoA dehydrogenase/3-ketoacyl-CoA thiolase/enoyl-CoA hydratase (trifunctional protein), alpha subunit	HADHA	Q64428	17.67	10.24	-1.73
Prostaglandin E synthase 3 (cytosolic)	PTGES3	P83868	2.39	1.42	-1.69
Ubiquinol cytochrome c reductase core protein 2	UQCRC2	P32551	5.31	3.18	-1.67
NADH dehydrogenase (ubiquinone) Fe-S protein 1	NDUFS1	Q66HF1	1.66	1.00	-1.66
Pyruvate dehydrogenase (lipoamide) alpha 2	PDHA2	Q06437	4.42	2.75	-1.61
Voltage-dependent channel 3	VDAC3	Q9R1Z0	9.11	5.69	-1.60
NADH dehydrogenase (ubiquinone) Fe-S protein 4	NDUFS4	Q5XIF3	1.68	1.10	-1.53

been capable of repairing damage incurred and that the spermatogonia initially exposed were not irreversibly affected. Interestingly, not all aspects of chromatin structure returned to normal status after the 9-wk recovery period. The observation that protamination, as evaluated by the CMA3 assay, and protamine protein expression levels, as determined using immunofluorescence, were significantly and specifically decreased only after a prolonged cessation of the BEP treatment lead us to propose that there was persistent damage in BEP-treated spermatozoa. A phenotypic change in sperm heads with DNA in a more open and decondensed confirmation was expected. Therefore, using Metamorph Imaging System analysis software, both the area and perimeter of protamine 1 staining, found within the entire sperm nucleus and thus a comparable indicator of the area and perimeter of the complete sperm head, were assessed. Although there was a clear trend toward an increase in both parameters in the treatment group,

these differences were not statistically significance for either parameter (see Supplemental Figure S2A).

Since protamine is one of the main proteins found in the head of spermatozoa and is in close association with DNA, a change in its expression after recovery from BEP treatment led to the hypothesis that other sperm head proteins that are important for normal sperm function may also be affected. In addition to changes in sperm chromatin structure, exposure of rats to cyclophosphamide led to concomitant modifications in the sperm basic proteome and nuclear matrix proteins [23, 27]. Several studies have also reported alterations in rat sperm protein profiles after exposure to various chemicals [28, 29]. Furthermore, the transcriptome of round spermatids following BEP treatment is modified extensively, with a specific increase in genes involved in stress response pathways [15].

The proteomic analysis we undertook of rat sperm heads was minimally contaminated with several abundant tail proteins, as seen in Supplemental Table S2, possibly masking

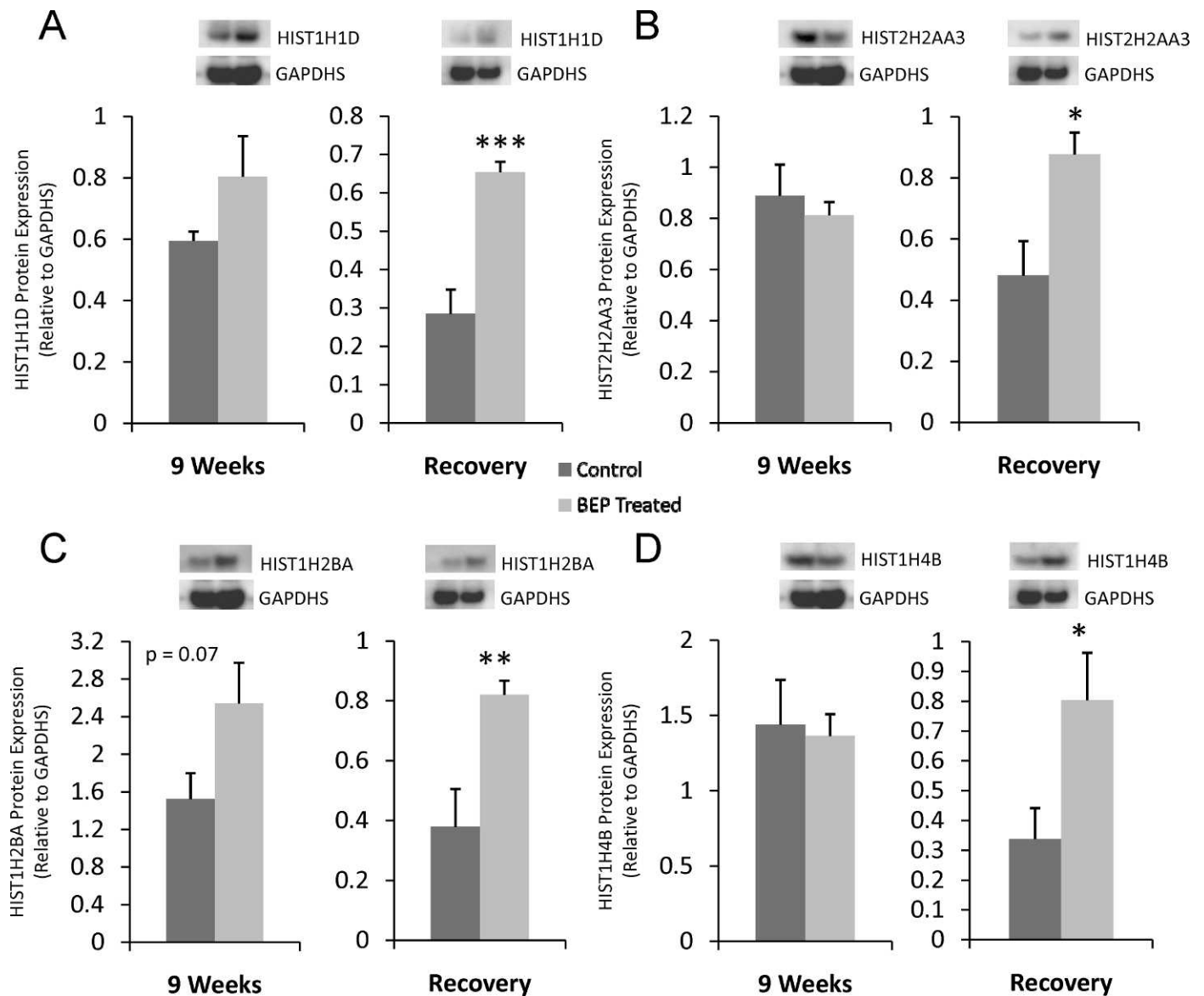


FIG. 5. Effects of BEP treatment at 9 wk and following a 9-wk recovery period on histone protein levels: HIST1H1D (H1.2) (A), HIST2H2AA3 (H2A1) (B), HIST1H2BA (H2B1A) (C), and HIST1H4B (H4) (D) in cauda spermatozoa. Bars represent means \pm SEM. (* $P < 0.05$), (** $P < 0.01$), and (***) $P < 0.001$, $n = 5-6$.

the identification of lower-abundance sperm head proteins; however, our results showed a change in their protein profiles for animals treated for 9 wk with BEP. Surprisingly, a greater number of proteins was significantly changed in spermatozoa of rats in the recovery group when compared to spermatozoa of animals immediately following the 9 wk of treatment. This increase may be the result of activation of compensatory mechanisms necessary to repair damage sustained in the cells after treatment. Interestingly, two proteins, heat shock protein 90, beta, member 1 (HSP90B1), and heat shock protein 90, alpha (cytosolic), class A, member 1 (HSP90AA1), were found to be up-regulated after 9 wk of BEP treatment and remained elevated in the animals following 9 wk of recovery. Both of these proteins are chaperones with well-characterized roles in protein-folding and in the assembly of multimeric protein complexes; however, recent evidence demonstrating that both proteins are tyrosine phosphorylated during sperm capacitation and mediate sperm-zona pellucida interactions highlights an

important role for these protein in fertilization events [30, 31] and may explain their up-regulation.

One of the predominant changes observed in the proteomic analyses was an up-regulation of histones in the sperm head of animals treated with BEP for 9 wk followed by a 9-wk recovery period. The up-regulated histones are histone H1.2, a testis-specific variant known as histone H2B1A, histone H2A1, and histone H4. H4 up-regulation in spermatozoa of animals treated with BEP followed by a recovery period was confirmed using Western blots despite the lack of significance predicted from the proteomic analysis (Table 1). The identification of a specific protein by MS occurs in the femtomole range, whereas in a Western blot, protein detection with specific antibodies and ECL reagents requires only a few hundred molecules [32]. MS is capable of identifying many proteins at once but is limited to a relative quantification method, whereas Western blots represent a more absolute quantification method.

The change in the histone to protamine ratio detected in spermatozoa after recovery from BEP treatment may be a result

of histone transcripts being translated at a higher frequency, leading to the up-regulation of these proteins, or due to a failure to displace the histones during spermiogenesis and replace them with transition proteins and protamines. If the latter is the explanation for this observation, the retention of specific histones may occur in response to the drug treatment, such that the DNA is poised for specific gene expression patterns. Recent evidence has shown that the retained nucleosomes in human sperm are enriched at loci particularly important for embryo development [33]. Additionally, it was noted that precise histone modifications were localized to particular developmental loci. Whether histones that are present in sperm after the BEP recovery phase are modified posttranscriptionally and whether they have an effect on particular gene expression loci have yet to be elucidated.

The effects of BEP chemotherapy on fertility and progeny outcome were at least partially reversible since no significant differences in the rate of postimplantation loss or the number of pups per litter were observed in litters sired by animals 9 wk posttreatment [34]. However, preimplantation loss remained elevated in litters sired by BEP-treated animals after a 9-wk recovery period [34]. Persistent preimplantation loss may be a protective mechanism to prevent the development of unhealthy embryos and may be due to residual damage that remained in germ cells following exposure. Of the pups that survived, analysis of their sperm protamine and histone content would be essential to determine if epigenetic modification were heritably propagated to subsequent generations, along with potential changes to fertility and progeny outcome.

To the best of our knowledge, no other studies have reported a change in histone content following a drug treatment, nor have there been any studies that have done a proteomic analysis solely on the rat sperm head to quantify changes in protein expression after exposure to any xenobiotic. Proteomic analysis, describing the proteome of rat spermatozoa as a whole cell, including head and tail fractions, has been reported previously [35], in addition to a two-dimensional fluorescence difference gel electrophoresis analysis of spermatogenesis, identifying proteins specifically or preferentially expressed at each stage of rat spermatogenesis [36]. Several other recent studies have used a proteomics approach to understand the mechanism by which sperm acquire fertilization capacity during epididymal maturation [37, 38].

In conclusion, our findings demonstrate that following recovery from treatment with BEP, DNA strand breaks are reduced, but persistent damage remains in the chromatin structure of spermatozoa. Future studies are required to determine whether the alterations in protamine and histone content in these spermatozoa result in heritable epigenetic modifications in progeny sired from paternally exposed males.

ACKNOWLEDGMENT

We wish to thank McGill University and Genome Quebec Innovation Centre for their technical assistance with the proteomic methodology, Ken McDonald (McGill University) for assistance with flow cytometry, as well as McGill University's Imaging Facility for their help in image acquisition and analysis.

REFERENCES

- Bray F, Richiardi L, Ekbom A, Pukkala E, Cuninkova M, Moller H. Trends in testicular cancer incidence and mortality in 22 European countries: continuing increases in incidence and declines in mortality. *Int J Cancer* 2006; 118:3099–3111.
- Huyghe E, Matsuda T, Thonneau P. Increasing incidence of testicular cancer worldwide: a review. *J Urol* 2003; 170:5–11.
- Robinson D, Moller H, Horwich A. Mortality and incidence of second cancers following treatment for testicular cancer. *Br J Cancer* 2007; 96:529–533.
- Einhorn LH, Foster RS. Bleomycin, etoposide, and cisplatin for three cycles compared with etoposide and cisplatin for four cycles in good-risk germ cell tumors: is there a preferred regimen? *J Clin Oncol* 2006; 24:2597–2598; author reply 2598–2599.
- Huddart RA, Birtle AJ. Recent advances in the treatment of testicular cancer. *Expert Rev Anticancer Ther* 2005; 5:123–138.
- Kopp HG, Kuczyk M, Classen J, Stenzl A, Kanz L, Mayer F, Bamberg M, Hartmann JT. Advances in the treatment of testicular cancer. *Drugs* 2006; 66:641–659.
- Bieber AM, Marcon L, Hales BF, Robaire B. Effects of chemotherapeutic agents for testicular cancer on the male rat reproductive system, spermatozoa, and fertility. *J Androl* 2006; 27:189–200.
- Delbes G, Hales BF, Robaire B. Toxicants and human sperm chromatin integrity. *Mol Hum Reprod* 2010; 16:14–22.
- Braun RE. Packaging paternal chromosomes with protamine. *Nat Genet* 2001; 28:10–12.
- Gatewood JM, Cook GR, Balhorn R, Bradbury EM, Schmid CW. Sequence-specific packaging of DNA in human sperm chromatin. *Science* 1987; 236:962–964.
- Balhorn R, Gledhill BL, Wyrobek AJ. Mouse sperm chromatin proteins: quantitative isolation and partial characterization. *Biochemistry* 1977; 16:4074–4080.
- Carrell DT, Hammoud SS. The human sperm epigenome and its potential role in embryonic development. *Mol Hum Reprod* 2010; 16:37–47.
- Aoki VW, Liu L, Jones KP, Hatasaka HH, Gibson M, Peterson CM, Carrell DT. Sperm protamine 1/protamine 2 ratios are related to in vitro fertilization pregnancy rates and predictive of fertilization ability. *Fertil Steril* 2006; 86:1408–1415.
- Singleton S, Mudrak O, Morshedi M, Oehninger S, Zalenskaya I, Zalensky A. Characterisation of a human sperm cell subpopulation marked by the presence of the TSH2B histone. *Reprod Fertil Dev* 2007; 19:392–397.
- Delbes G, Chan D, Pakarinen P, Trasler JM, Hales BF, Robaire B. Impact of the chemotherapy cocktail used to treat testicular cancer on the gene expression profile of germ cells from male Brown-Norway rats. *Biol Reprod* 2009; 80:320–327.
- Haines G, Marples B, Daniel P, Morris I. DNA damage in human and mouse spermatozoa after in vitro-irradiation assessed by the comet assay. *Adv Exp Med Biol* 1998; 444:79–91; discussion 92–93.
- Singh NP, Danner DB, Tice RR, McCoy MT, Collins GD, Schneider EL. Abundant alkali-sensitive sites in DNA of human and mouse sperm. *Exp Cell Res* 1989; 184:461–470.
- Delbes G, Hales BF, Robaire B. Effects of the chemotherapy cocktail used to treat testicular cancer on sperm chromatin integrity. *J Androl* 2007; 28:241–249; discussion 250–251.
- Evenson DP, Larson KL, Jost LK. Sperm chromatin structure assay: its clinical use for detecting sperm DNA fragmentation in male infertility and comparisons with other techniques. *J Androl* 2002; 23:25–43.
- Evenson DP, Wixon R. Environmental toxicants cause sperm DNA fragmentation as detected by the Sperm Chromatin Structure Assay (SCSA). *Toxicol Appl Pharmacol* 2005; 207:532–537.
- Bianchi PG, Manicardi GC, Bizzaro D, Bianchi U, Sakkas D. Effect of deoxyribonucleic acid protamination on fluorochrome staining and in situ nick-translation of murine and human mature spermatozoa. *Biol Reprod* 1993; 49:1083–1088.
- Zubkova EV, Wade M, Robaire B. Changes in spermatozoal chromatin packaging and susceptibility to oxidative challenge during aging. *Fertil Steril* 2005; 84(suppl 2):1191–1198.
- Codrington AM, Hales BF, Robaire B. Exposure of male rats to cyclophosphamide alters the chromatin structure and basic proteome in spermatozoa. *Hum Reprod* 2007; 22:1431–1442.
- Aoki VW, Moskovtsev SI, Willis J, Liu L, Mullen JB, Carrell DT. DNA integrity is compromised in protamine-deficient human sperm. *J Androl* 2005; 26:741–748.
- Martinez-Heredia J, Estanyol JM, Ballesca JL, Oliva R. Proteomic identification of human sperm proteins. *Proteomics* 2006; 6:4356–4369.
- Zhu W, Smith JW, Huang CM. Mass spectrometry-based label-free quantitative proteomics. *J Biomed Biotechnol* 2010; 2010:840518.
- Codrington AM, Hales BF, Robaire B. Chronic cyclophosphamide exposure alters the profile of rat sperm nuclear matrix proteins. *Biol Reprod* 2007; 77:303–311.
- Auger J, Eustache F, Maceiras P, Broussard C, Chafey P, Lesaffre C, Vaiman D, Camoin L, Auer J. Modified expression of several sperm proteins after chronic exposure to the antiandrogenic compound vinclozolin. *Toxicol Sci* 2010; 117:475–484.

29. Klinefelter GR, Strader LF, Suarez JD, Roberts NL, Goldman JM, Murr AS. Continuous exposure to dibromoacetic acid delays pubertal development and compromises sperm quality in the rat. *Toxicol Sci* 2004; 81:419–429.
30. Asquith KL, Baleato RM, McLaughlin EA, Nixon B, Aitken RJ. Tyrosine phosphorylation activates surface chaperones facilitating sperm-zona recognition. *J Cell Sci* 2004; 117:3645–3657.
31. Ecroyd H, Jones RC, Aitken RJ. Tyrosine phosphorylation of HSP-90 during mammalian sperm capacitation. *Biol Reprod* 2003; 69:1801–1807.
32. Wilm M, Shevchenko A, Houthaeve T, Breit S, Schweigerer L, Fotsis T, Mann M. Femtomole sequencing of proteins from polyacrylamide gels by nano-electrospray mass spectrometry. *Nature* 1996; 379:466–469.
33. Hammoud SS, Nix DA, Zhang H, Purwar J, Carrell DT, Cairns BR. Distinctive chromatin in human sperm packages genes for embryo development. *Nature* 2009; 460:473–478.
34. Marcon L, Hales BF, Robaire B. Reversibility of the effects of subchronic exposure to the cancer chemotherapeutics bleomycin, etoposide, and cisplatin on spermatogenesis, fertility, and progeny outcome in the male rat. *J Androl* 2008; 29:408–417.
35. Baker MA, Hetherington L, Reeves G, Muller J, Aitken RJ. The rat sperm proteome characterized via IPG strip prefractionation and LC-MS/MS identification. *Proteomics* 2008; 8:2312–2321.
36. Rolland AD, Evrard B, Guitton N, Lavigne R, Calvel P, Couvet M, Jegou B, Pineau C. Two-dimensional fluorescence difference gel electrophoresis analysis of spermatogenesis in the rat. *J Proteome Res* 2007; 6:683–697.
37. Baker MA, Smith ND, Hetherington L, Pelzing M, Condina MR, Aitken RJ. Use of titanium dioxide to find phosphopeptide and total protein changes during epididymal sperm maturation. *J Proteome Res* 2011; 10: 1004–1017.
38. Suryawanshi AR, Khan SA, Gajbhiye RK, Gurav MY, Khole VV. Differential proteomics leads to identification of domain-specific epididymal sperm proteins. *J Androl* 2011; 32:240–259.